MHD FLOW AND HEAT TRANSFER FOR MAXWELL FLUID OVER AN EXPONENTIALLY STRETCHING SHEET WITH VARIABLE THERMAL CONDUCTIVITY IN POROUS MEDIUM

by

Vijendra SINGH[a] and Shweta AGARWAL[b]*

[a] Department of Applied Science, Moradabad Institute of Technology, Moradabad, Uttar Pradesh, India
[b] Department of Mathematics, Hindu College, Moradabad, Uttar Pradesh, India

Original scientific paper
DOI: 10.2298/TSCI120530120S

A numerical analysis is made to study magnetohydrodynamic flow and heat transfer for Maxwell fluid over an exponentially stretching sheet through a porous medium in the presence of non-uniform heat source/sink with variable thermal conductivity. The thermal conductivity is assumed to vary as a linear function of temperature. The governing partial differential equations are transformed into ordinary differential equations using similarity transformations and then solved numerically using implicit finite difference scheme known as Keller-box method. The effect of the governing parameters on the flow field, skin friction coefficient, wall temperature gradient (in prescribed surface temperature case), wall temperature (in prescribed heat flux case) and Nusselt number are computed, analyzed and discussed through graphs and tables. The present results are found to be in excellent agreement with previously published work of El Aziz and Magyari and Keller on various special cases of the problem.

Keywords**:** *Maxwell fluid, porous medium, exponentially stretching sheet, non-uniform heat source/sink, variable thermal conductivity*

Introduction

The flow of a non-Newtonian fluid over a stretching sheet has attracted considerable attention during the last two decades due to its vast applications in industrial manufacturing such as hot rolling, wire drawing, glass fiber and paper production, drawing of plastic films, polymer extrusion of plastic sheets and manufacturing of polymeric sheets. For the production of glass fiber/plastic sheets, thermo-fluid problem involves significant heat transfer between the sheet and the surrounding fluid. Sheet production process starts solidifying molten polymers as soon as it exits from the slit die. The sheet is then collected by a wind-up roll upon solidification. To improve the mechanical properties of the fiber/plastic sheet we use two ways, the extensibility of the sheet and the rate of cooling.

Many researchers [1-4] investigated the steady boundary layer flow of an incompressible viscous fluid over a linearly stretching plate and gave an exact similarity solution in a closed analytical form under various physical conditions. Vajravelu [5] and Cortell [6, 7] investigated the boundary layer flows over a non-linear stretching sheet. Sajid *et al.* [8] found the analytic solution for axisymmetric flow over a non-linear stretching sheet. Akyildiz and Siginer [9] have investigated the flow and heat transfer over a non-linear stretching sheet by

* Corresponding author; e-mail: shweta.agg2000@gmail.com

using Legendre spectral method. Van Gorder and Vajravelu [10] have given the flow geometries and the similarity solutions of the boundary layer equations for a non-linearly stretching sheet. The similarity solutions of the boundary layer equations for non-linearly stretching sheet have been found by Akyildiz *et al*. [11]. Kumaran and Ramanaiah [12] analyzed the problem of heat transfer by taking quadratic stretching sheet.

Magyari and Keller [13] were the first to consider the boundary layer flow due to an exponentially stretching sheet and they also studied the heat transfer in the flow by taking an exponentially varying wall temperature. Elbashbeshy [14] numerically examined the flow and heat transfer over an exponentially stretching surface considering wall mass suction. Khan and Sanjayanand [15] investigated the flow of viscoelastic fluid and heat transfer over an exponentially stretching sheet with viscous dissipation effect. Recently Mukhopadhyay and Gorla [16] studied the effects of partial slip on boundary layer flow past a permeable exponential stretching sheet.

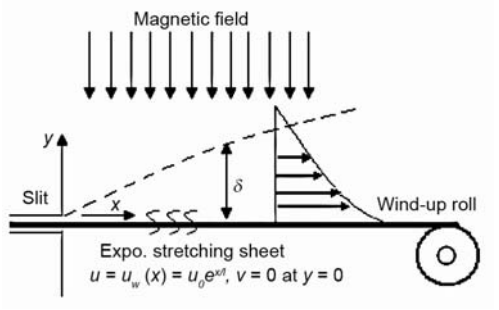

Figure 1. Physical configuration of the problem

Water is widely used fluid as the cooling medium, but for a better rate of cooling we have to control its viscoelasticity by using polymeric additives. If the fluid is electrically conducting, we can apply transverse magnetic field which alter the flow kinematics. Many researchers [4, 17, 18] have analyzed the influence of transverse magnetic field on the flow and heat transfer in an electrically conducting viscoelastic fluid over a linear stretching sheet. Singh and Agarwal [19] studied the effect of magnetic field on heat transfer for a second grade fluid over an exponentially stretching sheet with thermal radiation and elastic deformation.

In the rate of cooling, porous medium also plays a vital role. Eldabe and Mohamed [20] have obtained the solution for both heat and mass transfer in a magnetohydrodynamic (MHD) flow for a non-Newtonian fluid with a heat source over an accelerating surface through porous medium. The solution for the flow problem and heat transfer in a saturated porous medium has been obtained by Vajravelu [21]. Subhas and Veena [22] have studied the problem of viscoelastic fluid flow and heat transfer in a porous medium over a linear stretching sheet.

The rate of cooling also depends on the physical properties of the cooling medium but practical situation demands for physical properties with variable characteristics. Thermal conductivity is one of such properties, which is assumed to vary linearly with temperature. Some researchers [23-25] have studied the effect of variable thermal conductivity with temperature dependent heat source/sink. Eldahab and Aziz [26] have included the effect of non-uniform heat source with suction/bowling for viscous fluid only.

In recent years, flows of viscoelastic fluids over a linearly or exponentially stretching sheet (with and without heat transfer involved) have also been studied by some researchers. The theoretical studies cited above are important but are confined mainly to polymer industries due to the inherited shortcomings. Walters' B model and Second-grade model which are used in most studies are known to be good for weakly elastic fluids subject to slowly varying flow but the shortcoming for these fluids are that they violate certain rules of thermodynamics [27] and the work cited above for these fluids are based on boundary

layer theory which is still insufficient for non-Newtonian fluids. Obviously we use more realistic fluid to make the theoretical results to be of industrial significance. Maxwell model is one of such a fluid of industrial importance. Aliakbar *et al*. [28] investigate the influence of thermal radiation on MHD flow and heat transfer of Maxwellian fluid over a linear stretching sheet, but no attention has been made so far for Maxwellian fluid over an exponentially stretching sheet with variable thermal conductivity through porous medium as so far. In this paper we study the MHD flow and heat transfer for Maxwell fluid over an exponentially stretching sheet with variable thermal conductivity (Prandtl number is also varies with in the thermal boundary layer).

Basic equations

Flow equations

Consider, the steady 2-D boundary layer flow of an electrically conducting, viscoelastic fluid past a stretching sheet coinciding with the plane $y = 0$ (fig. 1) with the following two assumptions (for details see [13, 29]).

- The boundary sheet is assumed to be moving axially with a velocity of exponential order in the axial direction and generating the boundary layer type of flow.
- The normal stress is of the same order of magnitude as that of the shear stress, in addition to the usual boundary layer approximations.

Partha *et al*. [30] investigated the effect of viscous dissipation on the mixed convection heat transfer from an exponentially stretching surface. Nadeem *et al.* [31] studied the boundary layer flow of nanofluid and Nadeem and Lee [32] studied the boundary layer flow of Jeffrey fluid over an exponentially stretching surface. Boundary layer theory is more appropriate for Maxwell fluids in comparison to other viscoelastic fluids [28]. The boundary layer equations of conservation of mass and momentum for the MHD flow of an incompressible Maxwell fluid over an exponentially stretching sheet in usual notation can be written as [28]:

$$\frac{\partial u}{\partial x}+\frac{\partial v}{\partial y}=0 \tag{1}$$

$$u\frac{\partial u}{\partial x}+v\frac{\partial u}{\partial y}=\nu\frac{\partial^2 u}{\partial y^2}-\lambda\left[u^2\left(\frac{\partial^2 u}{\partial x^2}\right)+v^2\left(\frac{\partial^2 u}{\partial y^2}\right)+2uv\left(\frac{\partial^2 u}{\partial x\partial y}\right)\right]-\frac{\sigma B^2}{\rho}u-\frac{\nu u}{k'} \tag{2}$$

where u and v are velocity components in x- and y-direction, respectively, ν – the coefficient of kinematic viscosity, σ – the electrical conductivity of the fluid, ρ – the fluid density, B – the strength of magnetic field (applied in the transverse direction), and k' – the permeability of the porous medium. Here the magnetic Reynolds number is taken small and the induced magnetic field is neglected.

The boundary conditions for the flow are:

$$u=u_w(x)=u_0\mathrm{e}^{x/l},\ v=0 \ \text{ at } \ y=0 \text{ and } \ u=0 \text{ at } y\to\infty \tag{3}$$

where u_0 is a constant and l is the reference length.

Introducing the similarity transformation, to convert momentum equation from PDE to ODE:

$$\psi(x,y) = \sqrt{2\nu l u_0}\, F(x,\eta)\mathrm{e}^{x/2l} \tag{4}$$

where ψ is the stream function, F – the dimensionless stream function and:

$$\eta = y\sqrt{\frac{u_0}{2\nu l}}\mathrm{e}^{x/2l} \tag{5}$$

The velocity components u and v in terms of stream function $\psi(x, y)$ are $u = \partial\psi/\partial y$ and $v = \partial\psi/\partial y$, which satisfy the continuity eq. (1).

By using eqs. (4) and (5) in eq. (2), we do not find self-similar solution for the problem so we obtain local-similar solution of the problem by introducing a pseudo-similarity variable. In order to obtain local-similarity solution $F(x, \eta)$ should be assumed as $f(\eta)$ (for detail see [29]). We get a third order non-linear ODE:

$$2(f')^2 - ff'' + k^*\left[2(f')^3 + \frac{f^2 f'''}{2} - 3ff'f''\right] = f''' - 2f'(M+P) \tag{6}$$

where $k^* = \lambda u_0 \mathrm{e}^{x/l}/l$ is the local viscoelastic parameter, $P = \nu l/k' u_0 \mathrm{e}^{x/l}$ is the local porosity parameter, and $M = \sigma B^2 l/\rho u_0 \mathrm{e}^{x/l}$ is the local magnetic number.

The boundary conditions of flow in terms of f are:

$$f = 0, \quad f' = 1 \quad \text{at} \quad \eta = 0 \quad \text{and} \quad f' = 0 \quad \text{as} \quad \eta \to \infty \tag{7}$$

It should be pointed out that for $k^* = 0$ corresponds to that of Newtonian fluid.

The velocity components in terms of f are given as:

$$u = u_0 f' \mathrm{e}^{x/l} \quad \text{and} \quad v = -f\frac{\sqrt{2\nu l u_0}}{2l}\mathrm{e}^{x/2l} \tag{8}$$

Heat transfer equation

The governing boundary layer energy equation with variable thermal conductivity and non-uniform heat source/sink Q is given by:

$$\rho c_p\left(u\frac{\partial T}{\partial x} + v\frac{\partial T}{\partial y}\right) = \frac{\partial}{\partial y}\left(k\frac{\partial T}{\partial y}\right) + Q \tag{9}$$

where T is the temperature of the fluid, and c_p – the specific heat at constant pressure. Consider the thermal conductivity k varies linearly [23-25] with temperature and it is of the form:

$$k = \begin{Bmatrix} k_\infty[1 + \varepsilon\theta(\eta)] \text{ in PST case} \\ k_\infty[1 + \varepsilon g(\eta)] \text{ in PHF case} \end{Bmatrix} \tag{10}$$

where ε is a small parameter known as variable thermal conductivity parameter which is negative for solids and liquids and positive for gases [33], k_∞ – the thermal conductivity of the fluid far away from the sheet, $\theta(\eta)$ – a dimensionless temperature in prescribed surface temperature (PST) case, and $g(\eta)$ – the non-dimensional temperature in prescribed heat flux (PHF) case. The non-uniform heat source/sink Q [23] is modeled as:

$$Q = \frac{ku_w}{x\nu}\left[A^*(T_W - T_\infty)f' + (T - T_\infty)B^*\right] \tag{11}$$

where A^* and B^* are the coefficient of space and temperature dependent heat source/sink respectively, T_w is the wall temperature, and T_∞ – the temperature outside the dynamic region. Here $A^* > 0$, $B^* > 0$ shows internal heat generation and $A^* < 0$, $B^* < 0$ corresponds to internal heat absorption.

For solving energy eq. (9) we use two types of thermal boundary conditions.

(1) Prescribed surface temperature case

The boundary conditions in PST case is of the form:

$$T = T_w = T_\infty + A_1 e^{ax/2l} \text{ at } y = 0 \text{ and } T \to T_\infty \text{ as } y \to 0 \tag{12}$$

where A_1 and a are constants depends on the thermal properties of the liquid. $\theta(\eta)$ is a dimensionless temperature in PST case as:

$$\theta(\eta) = \frac{T - T_\infty}{T_w - T_\infty} \tag{13}$$

where

$$T - T_\infty = A_1 e^{ax/2l}\theta(\eta) \tag{14}$$

Using eqs. (10), (11), and (13) in eq. (9), we obtain the following non-linear ODE by taking $a = 2$:

$$(1 + \varepsilon\theta)\theta'' + \mathrm{Pr}_\infty f\,\theta' - 2\,\mathrm{Pr}_\infty f'\theta + \varepsilon\theta'^2 + (1 + \varepsilon\theta)(A^* f' + B^*\theta) = 0 \tag{15}$$

With the boundary conditions:

$$\theta(0) = 1, \quad \theta(\infty) \to 0 \tag{16}$$

where $\mathrm{Pr}_\infty = \mu c_p/k_\infty$ is the ambient Prandtl number and μ – the coefficient of viscosity. From the definition of Prandtl number, it is clear that this is a function of viscosity, thermal conductivity, and specific heat. In this paper thermal conductivity vary across the boundary layer, so Prandtl number also varies with in the boundary layer. The assumption of constant Prandtl number inside the boundary layer may produce unrealistic results [34-37]. Therefore, it must be treated as variable rather than a constant with in the boundary layer. Prandtl number related to the variable thermal conductivity is defined by:

$$\mathrm{Pr} = \frac{\mu c_p}{k}$$

and in PST case

$$\mathrm{Pr} = \frac{\mu c_p}{k_\infty\left[1 + \varepsilon\theta(\eta)\right]} = \frac{\mathrm{Pr}_\infty}{1 + \varepsilon\theta(\eta)}$$

$$\mathrm{Pr}_\infty = \mathrm{Pr}\left[1 + \varepsilon\,\theta(\eta)\right] \tag{17}$$

From eq. (17) it is clear that for small $\varepsilon(\varepsilon \to 0)$, $\mathrm{Pr} \to \mathrm{Pr}_\infty$ and for $\eta \to \infty$, $\theta(\eta)$ becomes zero therefore $\mathrm{Pr} = \mathrm{Pr}_\infty$. In light of the discussion by using eq. (17), the heat equation in PST case can be rewritten as:

$$(1+\varepsilon\theta)\theta'' + (1+\varepsilon\theta)\,\mathrm{Pr}\, f\,\theta' - 2(1+\varepsilon\theta)\,\mathrm{Pr}\, f'\theta + \varepsilon\theta'^2 + (1+\varepsilon\theta)(A^* f' + B^*\theta) = 0 \tag{18}$$

(2) Prescribed heat flux case

The boundary conditions in PHF case is of the form:

$$-k_\infty \left(\frac{\partial T}{\partial y}\right)_w = u_w = A_2 \mathrm{e}^{\left(\frac{b+1}{2l}\right)x} \quad \text{at} \quad y = 0 \quad \text{and} \quad T \to T_\infty \quad \text{as} \quad y \to \infty \tag{19}$$

where constants A_2 and b depends on the thermal properties of fluid. The non-dimensional temperature $g(\eta)$ in PHF case is defined as:

$$g(\eta) = \frac{T - T_\infty}{\frac{A_2}{k_\infty}\sqrt{\frac{2\nu l}{u_0}}\mathrm{e}^{bx/2l}} \tag{20}$$

Using eqs. (10), (11), and (20) in eq. (9), we obtain energy equation in terms of $g(\eta)$ as by taking $b = 2$:

$$(1+\varepsilon g)g'' + \mathrm{Pr}_\infty fg' - 2\,\mathrm{Pr}_\infty f'g + \varepsilon g'^2 + (1+\varepsilon g)(A^* f' + B^* g) = 0 \tag{21}$$

With the boundary conditions:

$$g'(0) = -\frac{1}{1+\varepsilon}; \quad g(\infty) \to 0 \tag{22}$$

As from PST case, the heat equation in PHF case in terms of variable Prandtl number is:

$$(1+\varepsilon g)g'' + (1+\varepsilon g)\,\mathrm{Pr}\, fg' - 2(1+\varepsilon g)\,\mathrm{Pr}\, f'g + \varepsilon g'^2 + (1+\varepsilon g)(A^* f' + B^* g) = 0 \tag{23}$$

Numerical procedure

The system of non-linear ODE (6) and (18) together with the boundary conditions (7) and (16) for the flow and heat transfer in PST case are solved numerically by using implicit finite difference method which is also known as Keller-box method [38, 39]. The numerical solutions are obtained using the following steps:

– reducing equations (6) and (18) to a system of first order equations;
– central differences are used to write the difference equations as:

$$2\left(\frac{\overline{f}_{i+1} - \overline{f}_{i-1}}{2h}\right)\left(\frac{f_{i+1} - f_{i-1}}{2h}\right) - \overline{f}_i\left(\frac{f_{i+1} - 2f_i + f_{i-1}}{h^2}\right) + 2k^*\left(\frac{\overline{f}_{i+1} - \overline{f}_{i-1}}{2h}\right)\left(\frac{\overline{f}_{i+1} - \overline{f}_{i-1}}{2h}\right)$$
$$\left(\frac{f_{i+1} - f_{i-1}}{2h}\right) + \frac{k^*}{2}\overline{f}_i\overline{f}_i\left(\frac{f_{i+2} - 2f_{i+1} + 2f_{i-1} - f_{i-2}}{2h^3}\right) - 3k^*\overline{f}_i\left(\frac{\overline{f}_{i+1} - \overline{f}_{i-1}}{2h}\right)\cdot$$
$$\cdot\left(\frac{f_{i+1} - 2f_i + f_{i-1}}{h^2}\right) = \left(\frac{f_{i+2} - 2f_{i+1} + 2f_{i-1} - f_{i-2}}{2h^3}\right) - 2(M+P)\left(\frac{f_{i+1} - f_{i-1}}{2h}\right) \tag{24}$$

$$\left(1+\varepsilon\bar{\theta}_i\right)\left[\left(\frac{\theta_{i+1}-2\theta_i+\theta_{i-1}}{h^2}\right)+\Pr\bar{f}_i\left(\frac{\theta_{i+1}-\theta_{i-1}}{2h}\right)-2\Pr\bar{\theta}_i\left(\frac{f_{i+1}-f_{i-1}}{2h}\right)+\right.$$

$$\left.+A^*\left(\frac{f_{i+1}-f_{i-1}}{2h}\right)+B^*\theta_i\right]+\varepsilon\left(\frac{\bar{\theta}_{i+1}-\bar{\theta}_{i-1}}{2h}\right)\left(\frac{\theta_{i+1}-\theta_{i-1}}{2h}\right)=0 \tag{25}$$

with the boundary conditions:

$$f_0=0,\quad \frac{f_1-f_{-1}}{2h}=1,\quad \frac{f_{n-1}-f_{n+1}}{2h}=0,\quad \theta_0=1,\quad \text{and}\quad \theta_n=0 \tag{26}$$

where the variables with bar are given arbitrary values from the previous steps:

– linearizing the algebraic equations by Newton's method, and writing them in matrix vector form;
– linear systems of equations are solved by Gauss-elimination technique.

To ensure the convergence of the numerical solution, numerical procedure have been applied in order to choose a suitable grid size $\Delta\eta = 0.001$, a suitable η range and a direct Gauss elimination technique with Newton's method is used in computer program to obtain solutions of these difference equations. Similarly we can solve eqs. (6) and (23) together with the boundary conditions (7) and (22) for the flow and the heat transfer in PHF case. The solutions are obtained with an error tolerance of 10^{-6} in all the cases.

Table 1. Values of skin friction $-f''(0)$ for different values of M, P, and k

M	P	k	$-f''(0)$
0.0	0.5	0.1	1.67091202
0.5			1.95296741
5			3.58074703
10			4.77728775
0.5	0.0	0.1	1.67091232
	0.5		1.95296741
	1.0		2.19466884
	2.0		2.61135409
0.5	0.5	0.0	1.91259405
		0.2	1.99244782
		0.6	2.14273251
		0.9	2.24854579

Results and discussions

To analyze the results, numerical computation has been carried out using the method described in the previous section for values of the local magnetic parameter M, local porosity parameter P, local viscoelastic parameter k, variable thermal conductivity parameter ε, variable Prandtl number, space dependent heat source/sink parameter A^*, and time dependent heat source/sink parameter B^*. For illustrations of the results numerical values are plotted in figs. 2-16. Results of skin friction coefficient $-f''(0)$ for selected values of local magnetic parameter M, local porosity parameter P, and local viscoelastic parameter k are listed in tab. 1. Results of $-\theta'(0)$ in PST case and $g(0)$ in PHF case for selected values of local magnetic parameter M, local porosity parameter P, local viscoelastic parameter k, variable thermal conductivity parameter ε, variable Prandtl number, space dependent heat source/sink parameter A^*, and time dependent heat source/sink parameter B^* are listed in tab. 2. In order to verify the accuracy of the present results, we have compared our results to those of previous works for some special cases. Table 3 presents a comparison of $-\theta'(0)$ in PST case among the results of El-Aziz [40] and Magyari *et al*. [13] and in the present study for different values of $\Pr_\infty$.

Table 2. Values of wall temperature gradient {-$\theta'(0)$} in PST case and wall temperature {$g(0)$} in PHF case for different values of physical parameters

M	P	k	ε	Pr	A^*	B^*	$-\theta'(0)$	$g(0)$
0.0	0.5	0.1	–0.1	3.0	0.05	0.05	2.38673459	0.47741446
0.5							2.30290418	0.49387801
5.0							1.80747360	0.62236517
10							1.49214410	0.74815032
0.5	0.0	0.1	–0.1	3.0	0.05	0.05	2.38673459	0.47741446
	0.5						2.30290418	0.49387801
	1.0						2.22854295	0.50952915
	2.0						2.09929318	0.53937418
0.5	0.5	0.0	–0.1	3.0	0.05	0.05	2.31272027	0.49188060
		0.2					2.29333904	0.50154144
		0.6					2.25729697	0.61051502
		0.9					2.23226802	0.52697411
0.5	0.5	0.1	–0.5	3.0	0.05	0.05	2.99837111	0.74701061
			–0.1				2.30290418	0.49387800
			0.0				2.21991332	0.45274802
			0.1				2.15296643	0.41764473
			0.5				1.97942131	0.31805478
0.5	0.5	0.1	–0.1	3.0	0.05	0.05	2.30290418	0.49387798
				4.0			2.75099817	0.41478409
				5.0			3.14349104	0.36366719
				7.0			3.82088948	0.29976386
0.5	0.5	0.1	–0.1	3.0	–0.5	0.05	2.48226132	0.46317934
					–0.2		2.38433515	0.47890095
					0.0		2.31917772	0.49071709
					0.2		2.25412152	0.50396457
					0.5		2.15672683	0.52806183
0.5	0.5	0.1	–0.1	3.0	0.05	–0.5	2.45883317	0.41914169
						–0.2	2.37648955	0.45991588
						0.0	2.31806142	0.48708677
						0.2	2.25580715	0.51424809
						0.5	2.15060672	0.55497202

Table 3. Comparison of – $\theta'(0)$ among El-Aziz [40], Magyari and Keller [13] and the present results in the PST case for different values of Pr_∞

k	M	Pr_∞	Magyari and Keller. [13]	El-Aziz [40]	Present results
0	0	1	0.954782	0.954785	0.95478372
		2			1.47148921
		3	1.869075	1.869074	1.86907634
		5	2.500135	2.500132	2.50013481
		10	3.660379	3.660372	3.66037773
0	1	1			0.53124395

Figures 2(a) and 2(b) show the profiles of velocity components u and v along x- and y-directions with in the viscoelastic boundary layer for different values of the local magnetic parameter M. It is clear from these figures that an increase in the local magnetic parameter M decreases stream-wise velocity component, u, and transverse velocity component, v, throughout the boundary layer flow field. It is because the application of transverse magnetic field will result in a resistive type force (Lorentz force which oppose the flow), similar to a drag force which tends to resist the fluid flow and thus reducing its velocity. The effect of local magnetic parameter M on the temperature profiles in both PST and PHF cases for the fluid is shown in figs. 3(a) and 3(b), respectively. It is evident from these figures that increase in the local magnetic parameter M also increases temperature profiles in both cases. This is due to the fact that Lorentz force tends to resist the flow and this resistance offered to the flow is responsible in broadening the thermal boundary layer thickness.

$$P = 0.5,\ k = 0.1,\ \varepsilon = -0.1,\ \mathrm{Pr} = 3.0,\ A^* = 0.05,\ B^* = 0.05$$

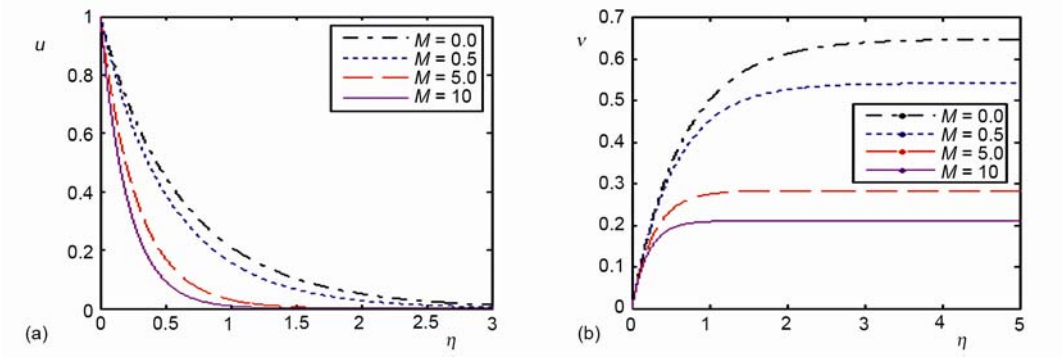

Figure 2. The effect of local magnetic number M on the u and v velocity components (*for color image see journal web-site*)

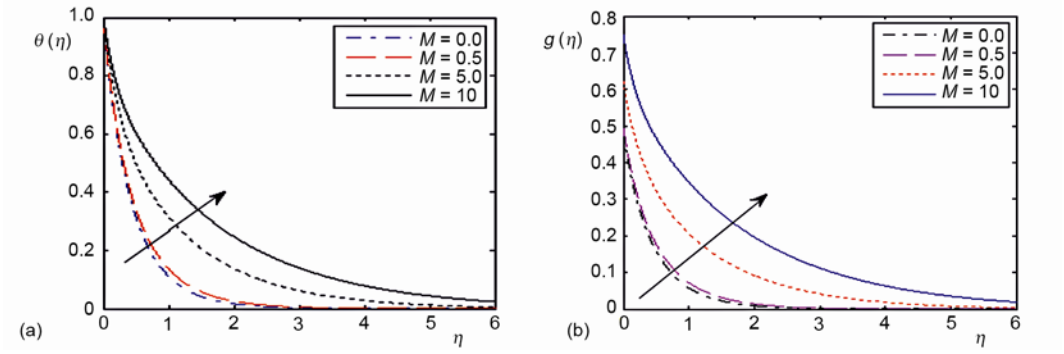

Figure 3. The effect of local magnetic number M on the temperature profiles in (a) PST and (b) PHF cases (*for color image see journal web-site*)

Figures 4(a) and 4(b) demonstrate the effect of local porosity parameter P on the velocity components, u and v. Like local magnetic parameter M, an increase in the local porosity parameter P the velocity components at any point decreases and temperature profiles in PST and PHF cases increase which is shown from figs. 5(a) and 5(b). We see that the non-dimensional wall temperature is unity in PST case and other than unity in PHF case for all parameters because of its differing boundary conditions.

$$M = 0.5,\ k = 0.1,\ \varepsilon = -0.1,\ \mathrm{Pr} = 3.0,\ A^* = 0.05,\ B^* = 0.05$$

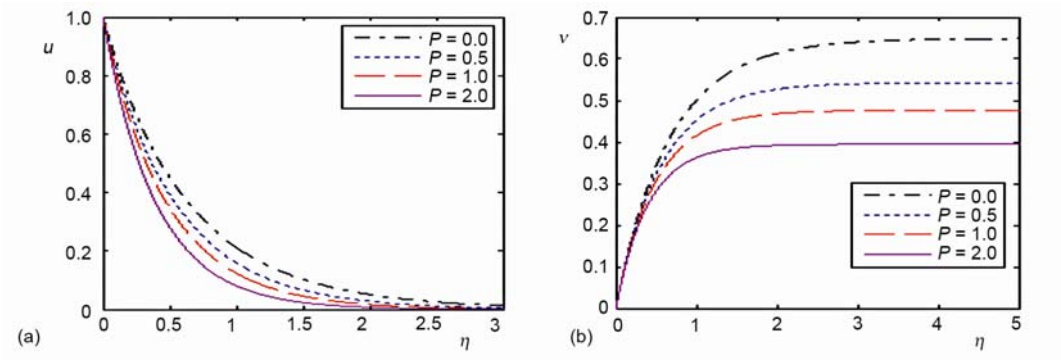

Figure 4. The effect of local porosity parameter *P* on the *u* and *v* velocity components (*for color image see journal web-site*)

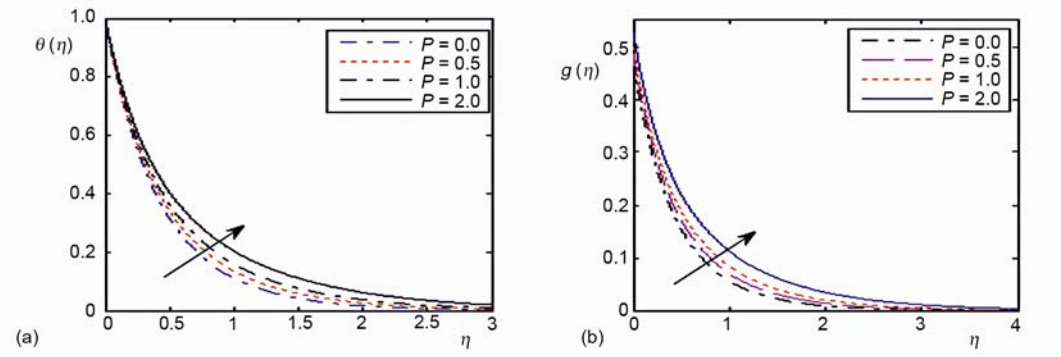

Figure 5. The effect of local porosity parameter *P* on the temperature profiles in (a) PST and (b) PHF cases (*for color image see journal web-site*)

Figures 6(a) and 6(b) show the effect of local viscoelastic parameter k on the velocity profiles above the sheet. An increase in the local viscoelastic parameter k is seen to decrease the velocity of the fluid element which is quite obvious. A decrease in the velocity component along x-direction means that the amount of heat transferred from the sheet to the fluid and a decrease in the velocity component along y-direction means the amount of fresh fluid which is extracted from the low-temperature region outside the boundary layer and directed towards sheet is reduced thus decreasing the amount of heat transfer.

The two effects are in the same directions reinforcing each other. The effect of local viscoelastic parameter k on temperature profiles in PST and PHF cases are shown in figs. 7(a) and 7(b), respectively. It is apparent from these figures the elasticity number increase fluid temperature at any given point above the sheet.

The effect of variable Prandtl number on temperature profiles in PST and PHF cases illustrate from figs. 8(a) and 8(b), respectively. In both cases, an increase in the value of variable Prandtl number is seen to decrease the temperature profiles because the thermal boundary layer becomes thinner to the large variable Prandtl number. The increase of variable Prandtl number means slow rate of thermal diffusion. Figures 9(a) and 9(b) demonstrate the effect of variable thermal conductivity parameter ε on the temperature profiles in PST and PHF cases,

respectively. In PST case, after increasing the value of variable thermal conductivity parameter ε temperature profiles also increases throughout the boundary layer but in PHF case, temperature profile decreases for small values of ε.

$$M = 0.5,\ P = 0.5,\ \varepsilon = -0.1,\ \mathrm{Pr} = 3.0,\ A^* = 0.05,\ B^* = 0.05$$

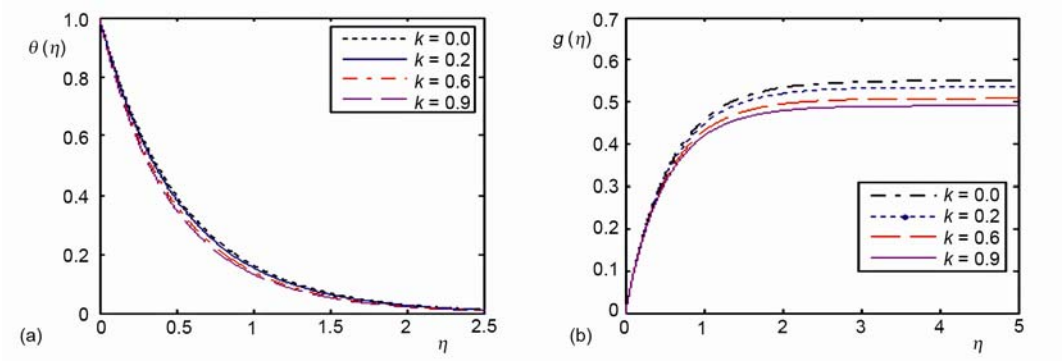

Figure 6. The effect of local viscoelastic number *k* on the *u* and *v* velocity components (*for color image see journal web-site*)

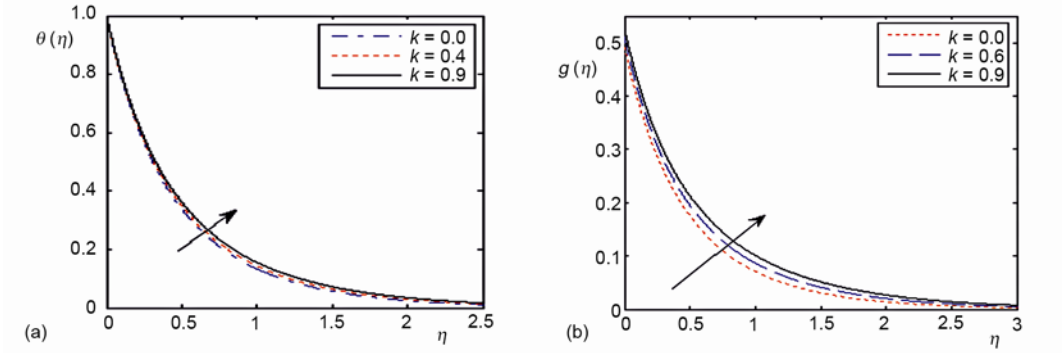

Figure 7. The effect of local viscoelastic number *k* on the temperature profiles in (a) PST and (b) PHF cases (*for color image see journal web-site*)

$$M = 0.5,\ P = 0.5,\ \varepsilon = -0.1,\ k = 0.1,\ A^* = 0.05,\ B^* = 0.05$$

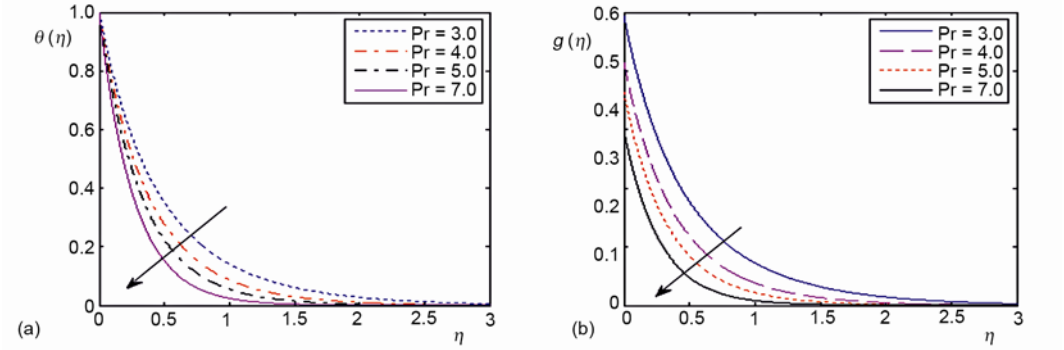

Figure 8. The effect of variable Prandtl number on the temperature profiles in (a) PST and (b) PHF cases (*for color image see journal web-site*)

$M = 0.5$, $P = 0.5$, $k = 0.1$, Pr = 3.0, $A^* = 0.05$, $B^* = 0.05$

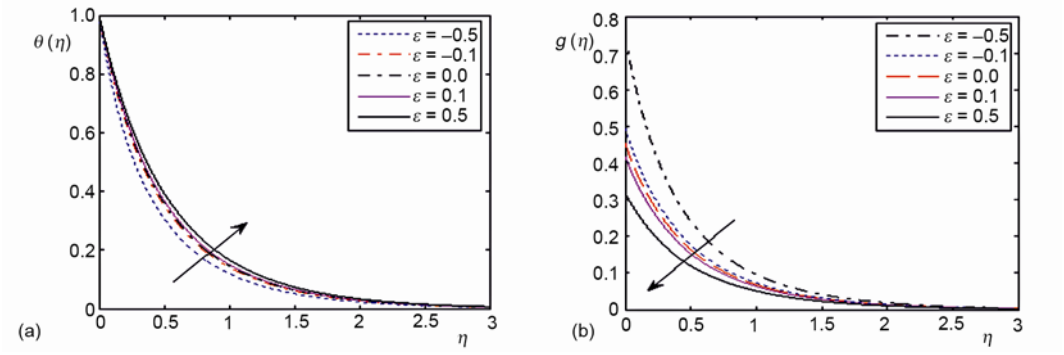

Figure 9. The effect of variable thermal conductivity parameter ε on the temperature profiles in (a) PST and (b) PHF cases (*for color image see journal web-site*)

Figures 10(a) and 10(b) show the graphical representation of temperature profiles with distance η for various values of space dependent heat source/sink parameter A^* in PST and PHF cases, respectively. It is apparent from these figures in the case of heat source ($A^* > 0$), the energy generated in thermal boundary layer causes the temperature profiles to increase with an increase in the value of A^*. On the other hand, for $A^* < 0$ (heat sink) the temperature $\theta(\eta)$ and $g(\eta)$ decreases with increasing the strength of the heat absorption. The effect of time dependent heat source/sink parameter B^* in PST and PHF cases for fluid is drawn in figs. 11(a) and 11(b), respectively. Like space dependent heat source/sink parameter A^* the temperature profile increases by increasing the values of time dependent heat source parameter B^* and decreasing the temperature profiles with increasing the strength of heat absorption.

$M = 0.5$, $P = 0.5$, $\varepsilon = -0.1$, Pr = 3.0, $k = 0.1$, $B^* = 0.05$

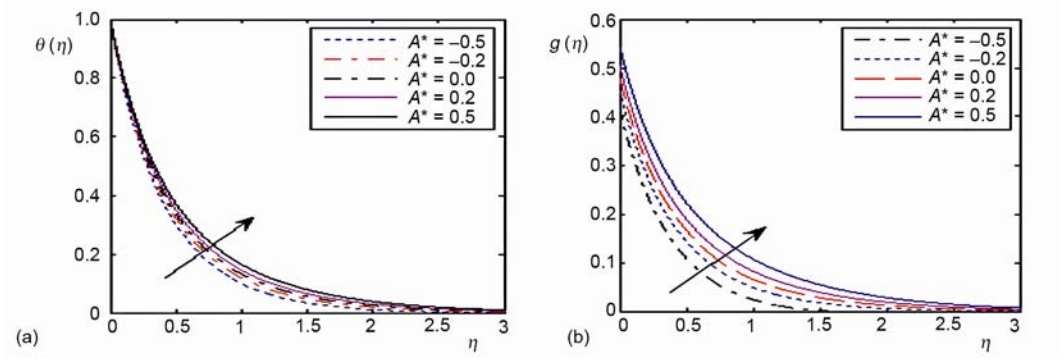

Figure 10. The effect of space dependent heat source/sink parameter A^* on the temperature profiles in (a) PST and (b) PHF cases (*for color image see journal web-site*)

Figures 12(a) and 12(b) demonstrate the graph of non-dimensional skin friction parameter C_{fx} *vs*. local viscoelastic parameter k for different values of the local magnetic parameter M and local porosity parameter P, respectively. From these figures it is clear that local viscoelastic parameter k leads to the decrease of skin friction parameter C_{fx}. This is because of that elasticity property in viscoelastic fluid reduces the frictional force. This result

$$M = 0.5,\ P = 0.5,\ \varepsilon = -0.1,\ \mathrm{Pr} = 3.0,\ k = 0.1,\ A^* = 0.05$$

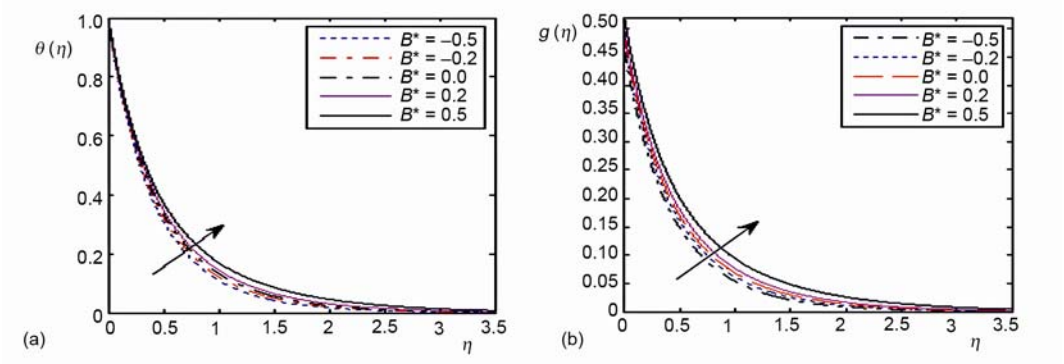

Figure 11. The effect of time dependent heat source/sink parameter B^* on the temperature profiles in (a) PST and (b) PHF cases (*for color image see journal web-site*)

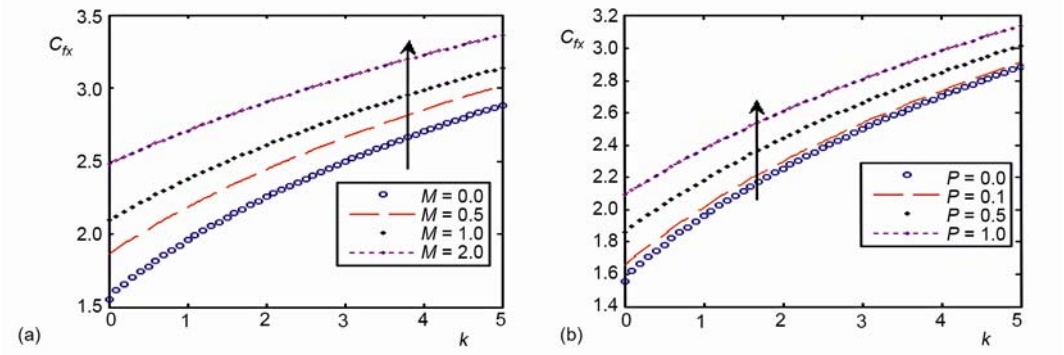

Figure 12. Variation of skin friction parameter C_{fx} *vs.* k for different values of (a) local magnetic number M with P = 0.5, and (b) local porosity parameter P with M = 0.5
(*for color image see journal web-site*)

may have great significance in polymer proceeding industry, as the choice of higher order viscoelastic fluid would reduce the power consumption for stretching the boundary sheet. We obtain the similar effect of local magnetic parameter M and local porosity parameter P on the skin friction coefficient as reduction of viscosity of the fluid in the decrease of frictional force or drag force.

The variations in Nusselt number, in terms of $-\theta'(0)$ in PST case and $1/g(0)$ in PHF case, with local viscoelastic parameter k for different values of local magnetic parameter M are presented in figs. 13(a) and 13(b), respectively. It is remarkable from these figures that increase in the local magnetic parameter M decreases Nusselt number in both cases. Moreover for given local magnetic parameter M the Nusselt number decreases with increasing the local viscoelastic parameter k. This is due to the fact that a larger local viscoelastic parameter k indicates more viscous fluid which decreases the fluid velocity and increase the fluid temperature.

Similarly, figs. 14(a) and 14(b) depict the variation of Nusselt number, with local viscoelastic parameter k for selected value of local porosity parameter P in PST and PHF cases, respectively. Like local magnetic parameter M, we get similar results for local porosity parameter P in both cases. The effects of local viscoelastic parameter k and variable Prandtl number on the Nusselt number are shown in figs. 15(a) and 15(b) for PST and PHF cases, re-

$$P = 0.5, A^* = B^* = \varepsilon = 0, \text{Pr} = 3.0$$

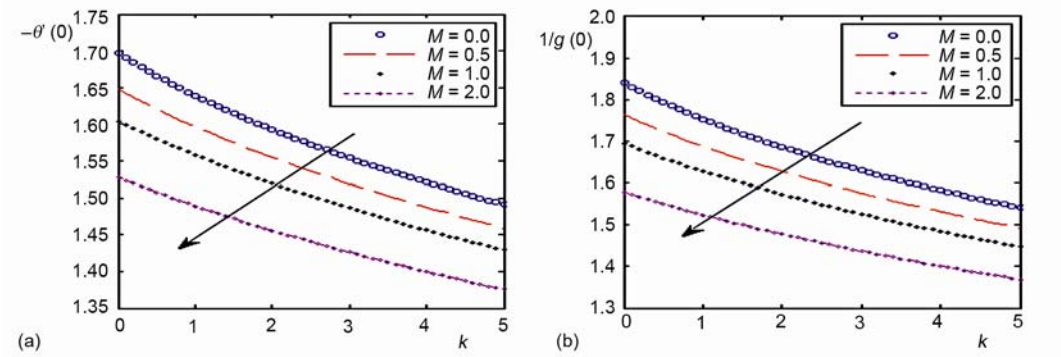

Figure 13. Variation of Nusselt number *vs. k* for different values of local magnetic number *M* (a) $-\theta'(0)$ in (a) PST case and (b) $1/g(0)$ in PHF case (*for color image see journal web-site*)

$$M = 0.5, A^* = B^* = \varepsilon = 0, \text{Pr} = 3.0$$

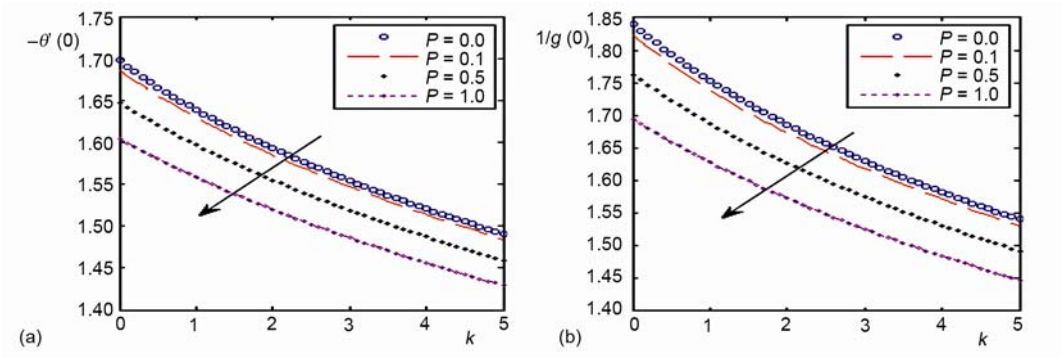

Figure 14. Variation of Nusselt number *vs. k* for different values of local porosity parameter *P* (a) $-\theta'(0)$ in PST case and (b) $1/g(0)$ in PHF case (*for color image see journal web-site*)

$$M = 0.5, P = 0.5, A^* = B^* = \varepsilon = 0$$

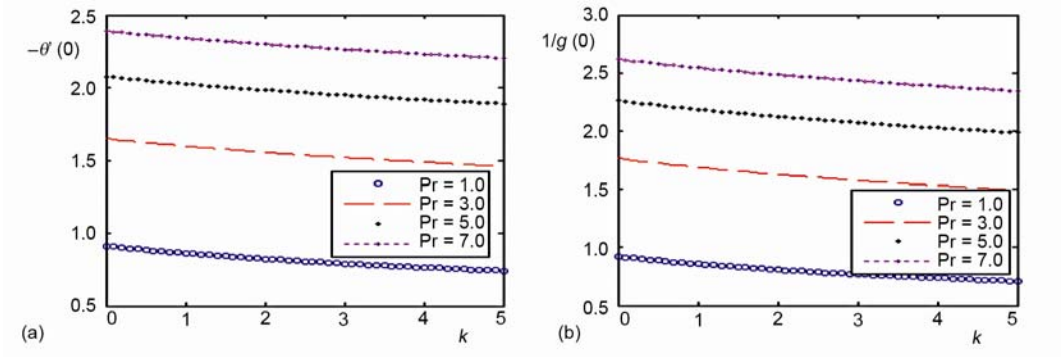

Figure 15. Variation of Nusselt number *vs. k* for different values of variable Prandtl number (a) $-\theta'(0)$ in PST case and (b) $1/g(0)$ in PHF case (*for color image see journal web-site*)

spectively. The effect of increment in variable Prandtl number is observed to increase the Nusselt number in both cases. This is because that fluid with larger variable Prandtl number has larger heat capacity, and thus enhances heat transfer. From these figures we also find that at given values of variable Prandtl number the values of $-\theta'(0)$ in PST case and $1/g(0)$ in PHF case increasing with increasing local viscoelastic parameter k.

Figures 16(a) and 16(b) display the variation of Nusselt number with local viscoelastic parameter k at the selected values of variable thermal conductivity parameter ε for PST and PHF cases, respectively. The effect of increasing variable thermal conductivity parameter ε is observed to decrease the Nusselt number in PST and PHF cases. The values of $-\theta'(0)$ in PST case and $1/g(0)$ in PHF case for a given values of variable thermal conductivity parameter ε, increasing with increasing local viscoelastic parameter k.

$$M = 0.5,\ A^* = B^* = 0,\ P = 0.5,\ \mathrm{Pr} = 3.0$$

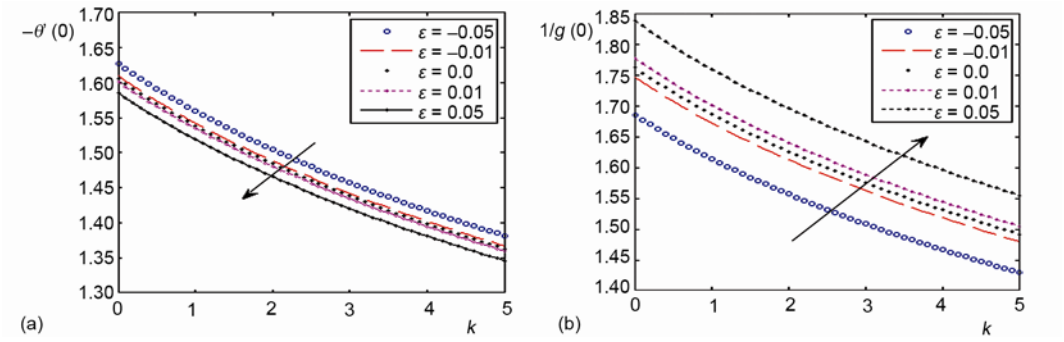

Figure 16. Variation of Nusselt number *vs. k* for different values of variable thermal conductivity parameter ε (a) $-\theta'(0)$ in PST case and (b) $1/g(0)$ in PHF case (*for color image see journal web-site*)

Conclusions

The important findings of this work are listed below.

- The effect of local magnetic parameter M and local porosity parameter P is found to decrease velocity and Nusselt number but increases the temperature profiles for both PST and PHF cases.
- Skin friction coefficient increases with local magnetic parameter M and local porosity parameter P.
- An increase in the local viscoelastic parameter k will produce a rise in the temperature profiles and decrease the velocity and Nusselt number for both PST and PHF cases.
- The effect of increasing the value of variable Prandtl number decreases the temperature of the fluid above the sheet and increases the Nusselt number for both PST and PHF cases.
- The increase in the variable thermal conductivity parameter ε increases the temperature of the fluid medium above the sheet in PST case but it behaves opposite in PHF case for small values of variable thermal conductivity parameter ε. The Nusselt number decreases for both the cases.
- The presence of space dependent heat source parameter ($A^* > 0$) or, time dependent heat source parameter ($B^* > 0$) causes an increase in the temperature profile but an opposite trend is observed for the case of space dependent heat sink parameter ($A^* < 0$) or, time dependent heat sink parameter ($B^* < 0$).

- Comparison of results of PST and PHF boundary conditions reveals that PHF is better suited for effective cooling of the stretching sheet.

Acknowledgments

The authors would like to thank the concerned reviewers for their valuable comments and also Council of Scientific and Industrial Research, New Delhi, for providing financial support through Grant No. 08/043(0005)/2008-EMR-1.

References

[1] Chen, C. K., Char, M. I., Heat Transfer of a Continuous Stretching Surface with Suction or Blowing, *J. Math. Anal. Appl., 135* (1988), 2, pp. 568-580
[2] Sakiadis, B. C., Boundary Layer Behaviour on Continuous Solid Surface: I – Boundary Layer Equations for Two Dimensional and Axisymmetric Flows, *AIChE. J., 7* (1961), 1, pp. 26-28
[3] Sakiadis, B. C., Boundary Layer Behaviour on Continuous Solid Surface: II – Boundary Layer on a Continuous Flat Surface, *AIChE. J., 7* (1961), 2, pp. 221-225
[4] Sarpakaya, T., Flow of Non-Newtonian Fluids in a Magnetic Field, *AIChE J., 7* (1961), 2, pp. 324-328
[5] Vajravelu, K., Viscous Flow over a Non-linearly Stretching Sheet, *Appl. Math. Comput., 124* (2011), 3, pp. 281-288
[6] Cortell, R., Viscous Flow and Heat Transfer over a Non-linearly Stretching Sheet, *Appl Math Comput, 184* (2007), 2, pp. 864-873
[7] Cortell, R., Effects of Viscous Dissipation and Radiation on the Thermal Boundary Layer over a Non-Linearly Stretching Sheet, *Phys. Lett. A, 372* (2008), 5, pp. 631-636
[8] Sajid, M., *et al*., Analytic Solution for Axisymmetric Flow over a Non-linearly Stretching Sheet, *Archive of Applied Mechanics, 78* (2008), 2, pp. 127-134
[9] Akyildiz, F. T., Siginer, D. A., Galerkin–Legendre Spectral Method for the Velocity and Thermal Boundary Layers over a Non-Linearly Stretching Sheet, *Non-linear Analysis: Real World Applications, 11* (2010), 2, pp. 735-741
[10] Van Gorder, R. A., Vajravelu, K., A Note on Flow Geometries and the Similarity Solutions of the Boundary Layer Equations for a Non-linearly Stretching Sheet, *Archive of Applied Mechanics, 80* (2010), 11, pp. 1329-1332
[11] Akyildiz, F. T., *et al*., Similarity Solutions of the Boundary Layer Equations for a Non-linearly Stretching Sheet, *Mathematical Methods in the Applied Sciences, 33* (2010), 5, pp. 601-606
[12] Kumaran, V., Ramanaiah, G., A Note on the Flow over a Stretching Sheet, *Acta Mech., 116* (1996), 1-4, pp. 229-233
[13] Magyari, E., Keller, B., Heat and Mass Transfer in the Boundary Layers on an Exponentially Stretching Continuous Surface, *J. Phys. D Appl. Phys., 32* (1999) 5, 577-585
[14] Elbashbeshy, E. M. A., Heat Transfer over an Exponentially Stretching Continuous Surface with Suction, *Arch. Mech., 53* (2001), 6, pp. 643-651
[15] Khan, S. K., Sanjayanand, E., Viscoelastic Boundary Layer Flow and Heat Transfer over an Exponentially Stretching Sheet, *Int. J. Heat Mass Transfer, 48* (2005), 8, pp. 1534-1542
[16] Mukhopadhyay, S., Gorla, R. S. R., Effects of Partial Slip on Boundary Layer Flow past a Permeable Exponential Stretching Sheet in Presence of Thermal Radiation, *Heat and Mass Transfer, 48* (2012), 10, pp. 1773-1781
[17] Andersson, H. I., MHD Flow of a Viscoelastic Fluid past a Stretching Surface, *Acta Mech., 95* (1992), 1-4, pp. 227-230
[18] Siddheshwar, P. G., Mahabaleshwar, U. S., Effect of Radiation and Heat Source on MHD Flow of a Viscoelastic Liquid and Heat Transfer over a Stretching Sheet, *Int. J. Non-Linear Mech., 40* (2005), 6, pp. 807-820
[19] Singh, V., Agarwal, S., Heat Transfer in a Second Grade Fluid over an Exponentially Stretching Sheet through Porous Medium with Thermal Radiation and Elastic Deformation under the Effect of Magnetic Field, *Int. J. Applied Mathematics and Mechanics, 8* (2012), 4, pp. 41-63
[20] Eldabe Nabil, T. M., Mohamed Mona, A. A., Heat and Mass Transfer in Hydromagnetic Flow of the Non-Newtonian Fluid with Heat Source over an Accelerating Surface through a Porous Medium, *Chaos, Solutions and Fractals, 13* (2002), 4, pp. 907-917

[21] Vajravelu, K., Flow and Heat Transfer in a Saturated Porous Medium, *ZAMM, 74* (1994), 12, pp. 605-614
[22] Subhas, A., Veena, P., Viscoelastic Fluid Flow and Heat Transfer in a Porous Medium over a Stretching Sheet, *Int. J. Non-linear Mech., 33* (1998), 3, pp. 531-540
[23] Abel, M. S., Mahesha, N., Heat Transfer in MHD Viscoelastic Fluid Flow over a Stretching Sheet with Variable Thermal Conductivity, Non-Uniform Heat Source and Radiation, *Appl. Math. Modelling, 32* (2008), 10, pp. 1965-1983
[24] Chiam, T. C., Heat Transfer with Variable Conductivity in a Stagnation-Point Flow towards a Stretching Sheet, *Int. Commun. Heat Mass Transfer, 23* (1996), 2, pp. 239-248
[25] Chiam, T. C., Heat Transfer in a Fluid with Variable Thermal Conductivity over a Linearly Stretching Sheet, *Acta Mech., 129* (1998), 2-3, pp. 63-72
[26] Eldahab, A. E. M., Aziz, M. A., Blowing/Suction Effect on Hydromagnetic Heat Transfer by Mixed Convection from an Inclined Continuously Stretching Surface with Internal Heat Generation/Absorption, *Int. J. of Therm. Sci. 43* (2004), 7, pp. 709-719
[27] Fosdick, R. L., Rajagopal, K. R., Anomalous Features in the Model of Second-Order Fluids, *Arch. Ration. Mech. Anal*., *70* (1979), 2, pp. 145
[28] Aliakbar, V., *et al.*, The Influence of Thermal Radiation on MHD Flow of Maxwellian Fluids above Stretching Sheets, *Comm. Non-Linear Sci. and Numerical simulation, 14* (2009), 3, pp. 779-794
[29] Sanjayanand, E., Khan, S. K., On Heat and Mass Transfer in a Viscoelastic Boundary Layer Flow over an Exponentially Stretching Sheet, *Int. J. Therm. Sci., 45* (2006) 8, pp. 819-828
[30] Partha, M. K., *et al*., Effect of Viscous Dissipation on the Mixed Convection Heat Transfer from an Exponentially Stretching Surface, *Heat and Mass Transfer, 41* (2005), 4, pp. 360-366
[31] Nadeem, S., *et al*., Effects of Thermal Radiation on the Boundary Layer Flow of a Jeffrey Fluid over an Exponentially Stretching Surface, *Numerical Algorithms, 57* (2011), 2, pp. 187-205
[32] Nadeem, S., Lee, C., Boundary Layer Flow of Nanofluid over an Exponentially Stretching Surface, *Nanoscale Research Letters, 7* (2012), 1, p. 94
[33] Nag, P. K., *Heat and Mass Transfer,* Tata Mc Graw Hill, New Delhi, India, 2008
[34] Rehman, M. M., *et al*., Heat Transfer in a Micropolar Fluid along a Non-Linear Stretching Sheet with a Temperature-Dependent Viscosity and Variable Surface Temperature, *Int. J. of Thermophysics, 30* (2009), 5, pp. 1649-1670
[35] Rehman, M. M., *et al*., Heat Transfer in Micropolar Fluid along an Inclined Permeable Plate with Variable Fluid Properties, *Int. J. Therm. Sci., 49* (2010). 6, pp. 993-1002
[36] Pantokratoras, A., Laminar Free-Convection over a Vertical Isothermal Plate with Uniform Blowing or Suction in Water with Variable Physical Properties, *Int. J. Heat Mass Transfer, 45* (2002), 5, pp. 963-977
[37] Pantokratoras, A., Further Results on the Variable Viscosity on Flow and Heat Transfer to a Continuous Moving Flat Plate, *Int. J. Eng. Sci., 42* (2004), 17, pp. 1891-1896
[38] Chapra, S. C., Canale, R. P., *Numerical Methods for Engineers,* Tata McGraw-Hill, New Delhi, India, 1990
[39] Keller, H. B., *Numerical Methods for Two-Point Boundary Value Problems*, Dower Publishing, New York, USA, 1992
[40] El-Aziz, M. A., Viscous Dissipation Effect on Mixed Convection Flow of a Micropolar Fluid over an Exponentially Stretching Sheet, *Can. J. Phys*., *87* (2009), 4, pp. 359-368

Paper submitted: May 30, 2012
Paper revised: August 2, 2013
Paper accepted: August 27, 2013